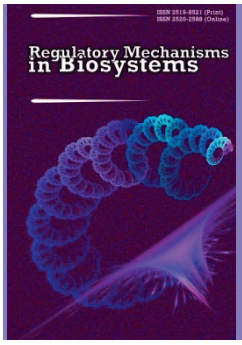


Regulatory Mechanisms in Biosystems

ISSN 2519-8521 (Print)
ISSN 2520-2588 (Online)
Regul. Mech. Biosyst.,
2022, 13(2), 180–188
doi: 10.15421/022223

# Multiscale oscillations of the annual course of temperature affect the spawning events of rudd (*Scardinus erythrophthalmus*)

O. M. Kunakh*, D. L. Bondarev**, N. L. Gubanova***, A. V. Domnich****, O. V. Zhukov*****

**Oles Honchar Dnipro National University, Dnipro, Ukraine*
***"Dnipro-Orylskiy" Nature Reserve, Obukhovka, Ukraine*
****Dnipro State Agrarian and Economic University, Dnipro, Ukraine*
*****Zaporizhzhia National University, Zaporizhzhia, Ukraine*
******Bogdan Khmelnitsky Melitopol State Pedagogical University, Melitopol, Ukraine*

*Article info*
*Received 06.04.2022*
*Received in revised form 03.05.2022*
*Accepted 04.05.2022*

*Oles Honchar Dnipro National University, Gagarin av., 72, Dnipro, 49000, Ukraine. Tel.: +38-098-858-23-79. E-mail: kunah_olga@ukr.net*

*"Dnipro-Orylskiy" Nature Reserve, Obukhovka, 52030, Dnipropetrovsk Region, Ukraine. Tel.: +38-066-745-14-62. E-mail: ihtio72log@ukr.net*

*Dnipro State Agrarian and Economic University, Sergey Efremov st., 25, Dnipro, 49600, Ukraine. Tel.: +38-067-751-71-02. E-mail: nlg2277@gmail.com*

*Zaporizhzhia National University, Zhukovsky st., 66, Zaporizhzhia, 69600, Ukraine. Tel.: +38-067-612-66-23. E-mail: domvidbio@gmail.com*

*Bogdan Khmelnitsky Melitopol State Pedagogical University, Hetmanska st., 20, Melitopol, 72318, Ukraine. Tel.: +38-098-507-96-82. E-mail: zhukov_dnipro@ukr.net*

***Kunakh, O. M., Bondarev, D. L., Gubanova, N. L., Domnich, A. V., & Zhukov, O. V. (2022). Multiscale oscillations of the annual course of temperature affect the spawning events of Rudd (Scardinus erythrophthalmus). Regulatory Mechanisms in Biosystems, 13(2), 180–188. doi:10.15421/022223***

Identifying climate impacts on ecosystems and their components requires observing time series of sufficient length to ensure adequate statistical power and reasonable coverage of the historical range of variability inherent in the system. The complexity of the hierarchy of climate effects reflected in temporal patterns in time series creates a need to be accurately modeled. The life cycle phenomena of living organisms, including fish spawning, have the character of one-time or time-limited events in time. An approach to finding the relationship between continuous components of time dynamics of environment properties and life cycle events of living organisms was proposed. This approach allowed us to evaluate the role of temperature patterns in the phenology of spawning rudd (*Scardinus erythrophthalmus* Linnaeus, 1758) in the Dnipro River basin water bodies. The atmospheric temperature time series may be decomposed into the following components: trend, annual cycle, episodic component, harmonic component, extreme events, and noise. Systematically low water temperatures at the beginning of the spawning period were observed in the Protoka River system and the Obukhov floodplain, and systematically elevated temperatures were recorded in the Dnipro River. The annual temperature dynamics was shown to be presented as a composition of oscillatory processes of different scale levels. The sinusoidal trend was previously extracted from the temperature series data. The average annual temperature, amplitude, and phase shift were calculated on the basis of the sinusoidal regression model. The residuals of the sinusoidal trend were processed by means of redundancy analysis with variables derived from symmetric distance-based Moran's eigenvector maps as explanatory predictors. A set of 104 orthogonal dbMEM variables was extracted from the annual time series. These temporal variables were divided into the broad-, medium-, and fine-scale components. The parameters of temperature dynamics and biotope type are able to explain 51–72% of variability of spawning event. The time of spawning in water bodies corresponds to the time of spawning start: the earlier spawning starts, the earlier it ends. The duration of the spawning season is influenced by the patterns of different scale levels, as well as the amplitude and shift of phases. In this case, the duration of spawning in all water bodies does not differ. Spawning temperature depends on medium- and fine-scale temperature patterns, but does not depend on the characteristics of the sinusoidal annual trend. The annual temperature variation has been shown to be such that it can be decomposed into a sinusoidal trend, patterns of a multiscale nature, and a random fraction. Over the time range studied, the trend of increasing mean annual temperature was not statistically significant for spawning events. The sinusoidal trend explains 78.3–87.6% of the temperature variations and depends on the mean annual temperature, the amplitude of temperature variations during the year, and the earlier or later seasons of the year. Amplitude and phase shift play a role in describing spawning phenology. The residuals of the sinusoidal trend have been explained using dbMEM variables. This variation was decomposed into large-scale, medium-scale, and small-scale components. Winter and spring temperature fluctuations prior to spawning initiation had the greatest effect on spawning. Water temperature determines the lower possible limit for the start of spawning, but the actual start of spawning is determined by the preceding temperature dynamics. The results of the study have implications for understanding the dynamics of fish populations and assessing the influence of environmental conditions on the harmonization of the various components of ecosystems.

*Keywords*: temporal pattern; phenology; climate change; oscilation dynamic; hierahy; temporal scales; biological rhythm.

## Introduction

A complex system such as an ecosystem can be decomposed into structural patterns and processing mechanisms that can be defined over a specific range of spatial and temporal scales (Allen et al., 2014). Small-scale observations are an essential way to study ecosystem dynamics (Cooper et al., 1998). The hierarchical structure of the ecological system reveals the fact that the patterns manifest themselves at the fixed scale, while the mechanism underlying this pattern acts at the different scales of space and time (Levin, 1992). That is why it is very important to understand how the patterns and changes observed at finer scales are reflected by those that occur at broader spatiotemporal scales. In an analogous way, it is important to understand how broad-scale processes correspond to the fine-scale phenomena (Scheffer & Van Nes, 2007; Nash et al., 2014). Every organism is an "observer" of the environment's hierarchical structure, and the life history adaptations alter the perceptual scales of the spe-

cies, and the observed environment heterogeneity (Levin, 1992). Climatic variability is increasingly considered to be a major structural factor affecting function and productivity in ecosystems (McGowan et al., 1998; Chavez et al., 2003; Avtaeva et al., 2021). The temperature of the water environment is a crucial driver of fish life cycle events (Brett, 1979; Herzig & Winkler, 1986; Jobling, 2003). The reproduction of many fish species is mainly controlled by temperature (Billard et al., 1978). Temperature affects the sex determination, gametogenesis dynamics, gametes' quality, fertility, age, sexual maturity and the duration of the reproductive season (Breton et al., 1980; Billard, 1986; Jafri, 1989; Sandstrom et al., 1995; Alavi & Cosson, 2005; Lahnsteiner & Mansour, 2012; Domagała et al., 2013). The changes in fish spawning time may be indicators of climate change (Schneider et al., 2010). The increased temperatures due to global warming are stimulating earlier spawning time for some fish species (Nõges & Järvet, 2005).

Identifying climatic impacts on ecosystems and their components requires observing time series of sufficient length to ensure adequate statistical power and reasonable coverage of the historical range of variability inherent in the system (Black et al., 2010). Statistical analysis of available time series showed the variation in distribution and abundance of fish species correlated with environmental variables (Weijerman et al., 2005). Species that significantly respond to recent increases in water temperature with shifts in range boundaries have faster life cycles and smaller body sizes (Perry et al., 2005). The complexityof the hierarchy of climate effects reflected in temporal patterns in time series creates a need to be accurately modeled (Kodba et al., 2005; Gao et al., 2011, 2012). The principal coordinates of neighbour matrix (PCNM) approach may be used for time series modelling by means of redundancy analysis, which is a form of canonical ordination (Angeler et al., 2009; Garcia et al., 2012). In the PCNM-approach a distance matrix converted from temporal coordinates is decomposed into the sinusoid components with different frequencies (Angeler et al., 2009). Due to redundancy analysis with PCNM-functions as explanation variables the relevant temporal patterns may be extracted and their explanatory strength may be evaluated (Borcard & Legendre, 2002). The PCNM-based approach was modified into distance-based Moran's eigenvector maps (MEM) (Dray et al., 2006), which are more robust in manipulating correlation structures and allow one to explain a higher proportion of variation compared to the original PCNM approach (Dray et al., 2006). The degree of fish community niche overlapping was revealed to be dependent on the broad-, medium-, and fine-scale patterns of the temperature variation derived due to MEM-procedure (Zhukov et al., 2019).

Thus, existing statistical techniques allow decomposition of time series of ecological variables. It should be noted that life cycle phenomena of living organisms, including fish spawning, have the character of one-time or time-limited events in time. And by definition, the time of occurrence of the same type of events is constantly changing year on year and in this situation it is not clear with what aspect of the environment properties to compare these biological events. Therefore, the question of how to find a relationship between continuous components of time dynamics of environment properties and life cycle events of living organisms, remains unsolved.

We propose the following hypotheses. 1. The annual temperature dynamics can be presented as a composition of oscillatory processes of different scale levels. 2. Temperature patterns of different scale levels may act as predictors of fish spawning events. Thus, the purpose of our study is to evaluate the role of temperature patterns in the phenology of spawning rudd (*Scardinus erythrophthalmus* Linnaeus, 1758) in the Dnipro River basin water bodies.

## Materials and methods

The native range of *S. erythrophthalmus* covers water bodies of Europe and Central Asia in the basins of the North, Baltic, Black, Caspian and Aral Seas (Berg, 1949). *Scardinus erythrophthalmus* inhabits a diversity of freshwater habitats, including oligotrophic lakes, lowland lakes, reservoirs, ponds, large rivers and streams (Kennedy & Fitzmaurice, 1974; Rheinberger et al., 1987). Spawning properties of this species depend on a number of factors. Sexual maturity reaches 2–3 years (Kennedy & Fitzmaurice, 1974) or 4 years of age (Boznak, 2008). The optimal age for spawning in males was 4 years and females 5 years (Patimar et al., 2010). In Ireland, *S. erythrophthalmus* spawn mainly from late May to early July, typically close to the shore (Kennedy & Fitzmaurice, 1974). In Poland *S. erythrophthalmus* begins to spawn when the water temperature reaches 14 °C in April, the spawning going on until June (Korzelecka & Winnicki, 1998). In colder areas of Poland, the spawning takes place from June until mid-July (Stehlik, 1968). In a lagoon located in the south-west of the Caspian Sea (Iran), this species spawned from mid April to the end of May, with a peak of spawning in mid-May (Patimar et al., 2010). In Turkey the spawning period for rudd occurs from early May to late June (Tarkan, 2006). The duration and timing of spawning is very diverse: in the conditions of the Dnipro Reservoir (Ukraine), spawning takes place in May–June (Bulakhov et al., 2008), in areas with more extreme climatic conditions (Syktyvkar, Russia) – from early June to early July (Boznak, 2008). In lakes in Catalonia (Spain), spawning takes place from mid May to mid August (Vila-Gispert & Moreno-Amich, 2000). In the UK, spawning of *S. erythrophthalmus* occurs at water temperatures between 14 °C and 23.5 °C, usually from late May to July (Kottelat & Freyhof, 2007). In the Dvina River basin, spawning occurs at temperatures above 11 ºC (Boznak, 2008). In Greece spawning begins at temperatures above 10 ºC (Papageorgiou & Neophytou, 1982). In the waters of Dagestan spawning occurs at temperatures 18–20 ºC (Shikhshabekov, 1979). In the Marmara region (Northwest Turkey) spawning occurs at temperatures 17.5–23.5 ºC. After spawning there is a 6-month quiescent period. A rapid growth of the gonads takes place during the period March–May. The ovaries of females were found to be developing from February to May. Males showed the same patterns as the females in terms of the maturity stages (Tarkan, 2006).

Temperature has a direct effect on the *S. erythrophthalmus* metabolism. The temperature below which the rudd has insufficient metabolic activity to produce growth is about 13 ºC (Zerunian et al., 1986). The rudd was shown experimentally to consume readily plant matter at water temperatures above 20 °C and avoids its consumption at temperatures below 20 °C. The field data indicate that in vivo plant matter dominates the rudd diets in summer and is absent in spring (Vejříková et al., 2016).

The materials that formed the basis of this research were collected from the waters of the "Dnipro-Orilskiy" Nature Reserve in the years 1997–2018. To obtain data on the characteristics and intensity of fish spawning we made visual observation and conducted planned survey routes through spawning grounds with stops every 20, 50, 100 m to check the vegetation and presence of fish eggs. If roe was found, the place of its location was described in detail. We noted the name of the water body, depth, water temperature, time of day, type of vegetation and richness of the spawning (Bondarev et al., 2022). As the spawning events the following observations were recorded : date of spawning start, date of spawning end, duration of spawning (per day), water temperature in the water body at the time of spawning start.

Information about fish spawning was collected in the following locations (Fig. 1).

The Nikolaev system of water bodies is a floodplain system, located in the narrowest part of the floodplain terraces. The pools extend in a narrow strip alongside the Dnipro River. The maximum distance from the Dnipro is about 300–1000 m. The reservoir system is characterized by high flow and water level difference during the day, depending on the reservoir operation conditions. The shallow waters (coastal zone) are minimal in area. The maximum depth is 5.6 m.

The Protoch River system and Obukhov floodplain is a shallow water system, which is the remnants of the lower part of the perforated stream, which united the Dnipro with the old course of the Orel. Most of the water bodies have a low current. The water regime of the Protoch system and the Obukhov floodplain is significantly influenced by the reservoir's water regime. The water bodies are characterized by significant silting (in some places, sludge thickness reaches 0.6–1.0 m) and growth of higher aquatic vegetation. The system is connected to the Dnipro and the estuary of the Oril by narrow streams. The largest distance between the Dnipro and the Oril at this section is about 2 km.

The channel of the Dnipro includes the territory of the Upper Dnipro Reservoir, which partially has a river regime. The study area is located

along the left bank of the Dnipro. The habitats are characterised by a high level of water level change and sand mass movement due to the active formation of the channel process at the reservoir site. The water depth varies between 2–7 m.

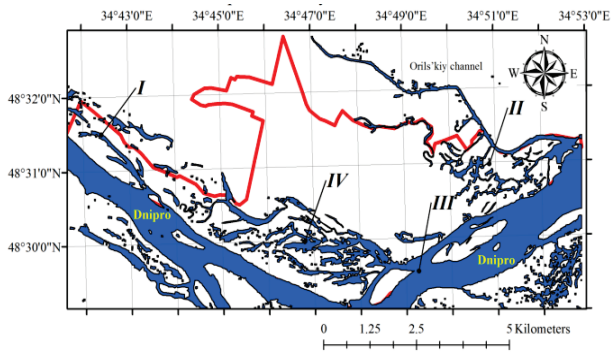


**Fig. 1.** Map of the "Dnipro-Orilskiy" Nature Reserve and spawning locations: *I* – Nikolaev system of water bodies; *II* –Protoch River system and Obukhov floodplain; *III* – the channel of the Dnipro River; *IV* – water bodies of the Taromske ledge

The water bodies of the Taromske ledge compose a floodwater system located in the lower part of floodplain terraces. All the lakes are separated from the Dnipro river bed by a sand belt and are connected by many channels directly linked to the Dnipro bed. Most of the lakes have a significant littoral zone, which is actively covered by higher aquatic vegetation. Depths vary between 1–10 m. Water is exchanged through the operation of the reservoir and spring floods. The maximum distance of these water bodies from the Dnipro is about two kilometers. At present, the ponds of this area are actively swamped and silted due to the unbalanced operation of the reservoir. In some areas, the thickness of silt reaches 0.3–0.7 m.

We used the data from the meteorological observatory of the city Dnipro. Meteorological data were obtained from the National Climatic Data Center (www.ncdc.noaa.gov) using the moaa package (Koshelev et al., 2021). In our work the time series of temperature from July 1 of the previous year to June 30 of the flow year (or June 29 of the flow high year) were considered as predictors of spawning events. In total, the duration of the time series was 365 days.

The atmospheric temperature time series may be decomposed into the following components: trend, annual cycle, episodic component, harmonic component, extreme events, and noise (Vislocky & Fritsch, 1995). A time series of one year duration includes only one annual cycle, so the linear trend is not represented in it. The MEM-approach requires detrending of the data to remove trends prior to analysis (Legendre & Legendre, 2012; Blanchet et al., 2013; Baho et al., 2015). To do this the sinusoidal trend was previously extracted from the temperature data (Fig. 2):

$$\text{Temperature} = a_0 + a_c\cos(2\pi\ \text{Time}/365) + a_s\sin(2\pi\ \text{Time}/365),$$

where Temperature is the fitted temperature value, Time is the number of days from 1 July of the previous year to June 30 of the current year. The amplitude of the sinusoidal process is $\sqrt{{a_c}^2 + {a_s}^2}$, and phase shift is $\text{atan}(a_s/a_c)$.

To summarize relationships among the residuals of the sinusoidal trend of the annual time series and dbMEM-variables, a redundancy analysis (RDA) was performed. RDA is a form of canonical ordination in which axes were restricted to linear combinations of the environmental variables (Borcard & Legendre, 2002; Legendre & Legendre, 2012). Symmetric distance-based Moran's eigenvector maps' analyses (MEM) (Dray et al., 2006a) were carried out to extract a set of orthogonal temporal variables (dbMEM-variables) that are derived from the time vector comprised of 360 time steps from July 1 of the previous year to June 30 of the current year. dbMEM-variables can be used as explanatory variables to model temporal patterns of the temperature courses. In MEM all variables depict sine-wave patterns (Legendre & Legendre, 2012). These extracted temporal variables are then used as explanatory variables in the time series models based on redundancy analysis (RDA). dbMEM-variables are linearly combined in the RDA models to extract temporal structures from the temperature time series. The significant RDA axes were tested through permutation tests. These RDA axes are independent from each other. The R software generates linear combination (lc) score which present the modelled temporal patterns that are associated with each RDA axis. The general linear models were used to test the significance of temeparature pattern effects on timing of spawning events.

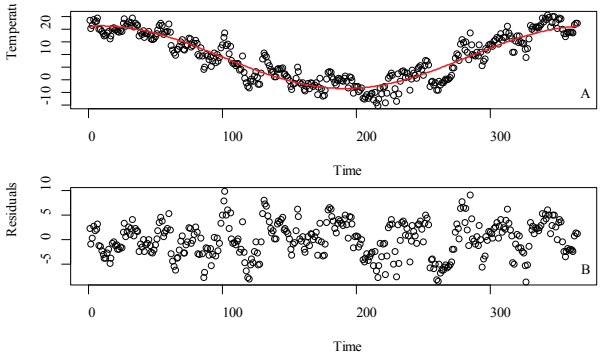


**Fig. 2.** Sinusoidal trend extracted from the temperature data: *a* – an annual course of the temperature, *b* – and residuals of the sinusoidal trend line, the abscissa axis is the number of days from 1 July of the previous year to June 31 of the current year, the ordinate axis is the temperature for the 1998 as example (*a*) and the residuals of the sinusoidal trend line (*b*), red line indicates the graph of the sinusoidal trend line which was fitted by the following equation: $\text{Temperature} = a_0 + a_1\cos(2\pi\ \text{Time}/365) + a_2\sin(2\pi\ \text{Time}/365)$, where Temperature is the fitted temperature value, Time is the number of days from 1 July of the previous year to June 30 of the current year

Statistical analyses were carried out in R 3.5.2 (R Development Core Team, 2018) using the following packages: vegan (v. 2.5-2, https://CRAN.R-project.org/package=vegan) for the multivariate analysis, adespatial (v. 0.3-2. https://CRAN.R-project.org/package=adespatial) for the forward selection and for the generation of temporal filters.

## Results

*Sinusoidal trend of temperature time series.* The sinusoidal component of the temperature time series is described by a regression with three parameters: the intercept of the regression equation, the coefficient of the cosine term of the regression equation, and the coefficient of the sine term of the regression equation (Fig. 3). The sinusoidal model is able to explain 78.3–87.6% of the annual temperature variation (Fig. 3a). The intersection represents the average annual air temperature in the study area. It is 9.5 ± 0.093 ºC and is in the range of 7.9–11.1 ºC. The mean annual temperature in the study area correlates with the order of years ($r = 0.41$, $P < 0.001$, Fig. 3b).

Average annual temperature is linked to the consequence of the years of linear regression:

$$T_a = 8.7 \pm 0.36 + 0.0574 \pm 0.028\ Y,$$

where $T_a$ – average annual temperature (ºC), Y – the order of the years from 1 – 1997, 2 – 1998, …, 22 – 2018. The P-value for coefficient of the slope term of the linear regression equation is 0.03 which reveals that this term is statistically significantly different from zero. Our results confirm a warming trend over the years 1997–2018. Neither the annual temperature amplitude (Fig. 3c) nor phase shift (Fig. 3d) calculated on the basis of the sinusoidal regression model correlates significantly with the order of years ($r = 0.27$, $P = 0.25$ and $r = 0.20$, $P = 0.39$ respectively).

*Multiscale decomposition of the trend residuals.* A set of 104 orthogonal dbMEM variables were extracted from the annual time series. These temporal variables are able to explain 72.7% ($F = 10.4$, $P < 0.001$) variation of the sinusoidal trend residuals. The scalogram exhibits the contribution into the variation explined by each dbMEM variable separately (Fig. 4). The first 18 dbMEM-variables were considered as a broad-scale component of the temperature variation. These variables explain 32.9% of total variation of the sinusoidal trend residuals ($F = 10.9$, $P < 0.001$). dbMEM-variables 19–40 were regarded as denoting the meso-scale component of the temperature variation. These variables explain 19.2% of total variation of the sinusoidal trend residuals ($F = 4.9$, $P < 0.001$). dbMEM-

variables 41–74 were regarded as denoting the fine-scale component of the temperature variation. These variables explain 5.8% of total variation of the sinusoidal trend residuals ($F = 1.65$, $P < 0.001$).

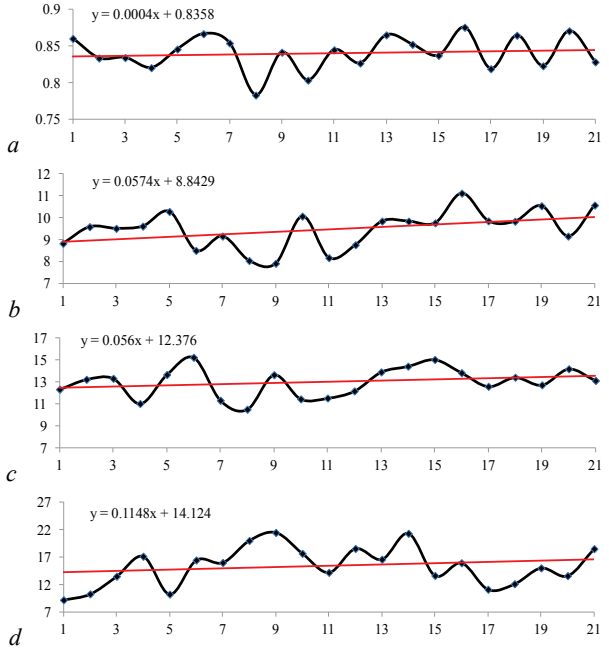


**Fig. 3.** The temporal dynamic of the sinusoidal trend parameters of the temperature annual course: *a* – the ordinate axis is the R2adj of sinusoidal regression model, *b* – the intercept of the regression equation or average annual temperature, ºC (B), *c* – the amplitude of the sinusoidal trend, *d* – and the phase shift of the sinusoidal trend, the abscissa axis is the order of years within the period 1998–2018: 1 – 1998, 2 – 1999, …, 21 – 2018

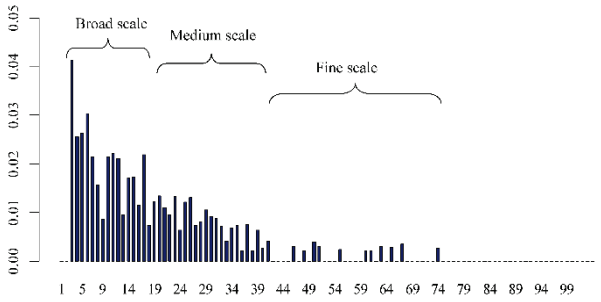


**Fig. 4.** Scalogram demonstrating the scaling of temporally structured variation in sinusoidal trend residuals data, the abscissa axis is the dbMEMs ordered decreasingly according to the scale of temporal patterns they represent (dbMEMs 1–18 represent the broad scale, dbMEMs 19–40 represent the medium scale and dbMEMs 41–74 represent the fine scale), the ordinate axis is the value of R2adj which is the variation explained by individual dbMEM variables

Constrained RDA of the sinusoidal trend residuals with broad-scale variables as predictors revealed three RDA-axes, which reflect the broad-scale patterns of annual temperature deviations from the typical temperature trend (Fig. 5). All three RDA-axes indicate the presence of abrupt temperature changes in a short time in winter. A sharp change in temperature manifests itself in cooling during 10–15 days (in case of positive axis value) or warming (in case of negative axis value). The differences between the axes are in what period of winter sharp changes in temperature occur. Broad-scale RDAb 1 is sensitive to changes in January, broad-scale RDAb 2 – in February and broad-scale RDAb 3 – in December.

The examination of the RDAb 1 values dynamics during the period of studies indicates that a sharp cold snap in January was observed in 2006 and 2012, and a sharp warming – in 2002 and 2009 (Fig. 6a). The dynamics of RDAb 2 demonstrates a sharp cold snap in February in 2011 and 2018 and a sharp warming in February 2010 (Fig. 6b). The dynamics of RDAb 3 shows a sharp cold snap in December 2003 and a sharp warming in December 1999 (Fig. 6c). Intermediate values of axes within amplitude indicate the degree of manifestation of corresponding paterns in other years.

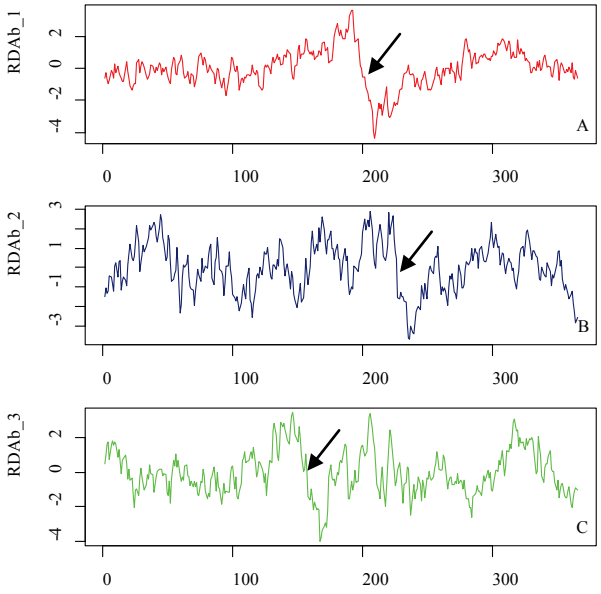


**Fig. 5.** The interannual dynamic of the scores of the broad-scale components RDAb 1–3: *a* – the ordinate axis is the scores of the broad-scale components RDAb 1, *b* – RDAb 2, *c* – RDAb 3, the abscissa axis is the years within the period 1998–2018, the arrows show the moment when the temperature changes abruptly

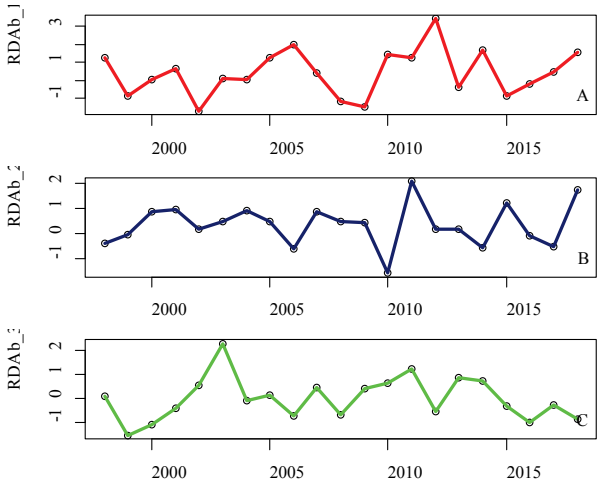


**Fig. 6.** The between annual dynamic of the scores of the broad-scale components RDAb 1–3: *a* – the ordinate axis is the scores of the broad-scale components RDAb 1, *b* – RDAb 2, *c* – RDAb 3, the abscissa axis is the years within the period 1998–2018, the arrows show the moment when the temperature changes abruptly

Constrained RDA of the sinusoidal trend residuals with meso-scale variables as predictors allowed us to extract three RDA-axis, which reflect the meso-scale patterns of annual temperature deviations from the sinisoidal temperature trend (Fig. 7). These axes reflect the presence of winter temperature dynamics, the time range with two consecutive drastic temperature changes. Meso-scale RDAm 1 indicates that this period takes place from mid-January to mid-February. Meso-scale RDAm 2 points out that this period is from December to mid-January. Meso-scale RDAm 3 reveals that sharp consecutive changes in temperature occur in January.

The dynamics of meso-scale RDAm 1 values suggest that two consecutive drastic temperature changes with two maximum and one minimum from mid-January to mid-February took place in 2007 and 2014 (Fig. 8a). In turn, in this period of the year the drastic temperature changes with one maximum and two minimum took place in 2006 (Fig. 8b). Ana-

logous changes in the temperature regime in December to mid-January took place in 2001, 2017, and 2018, and in January they took place in 2005 (Fig. 8c). We considered the most extreme examples. Axis values quantitatively characterize the degree of expression of the respective patterns in a given year.

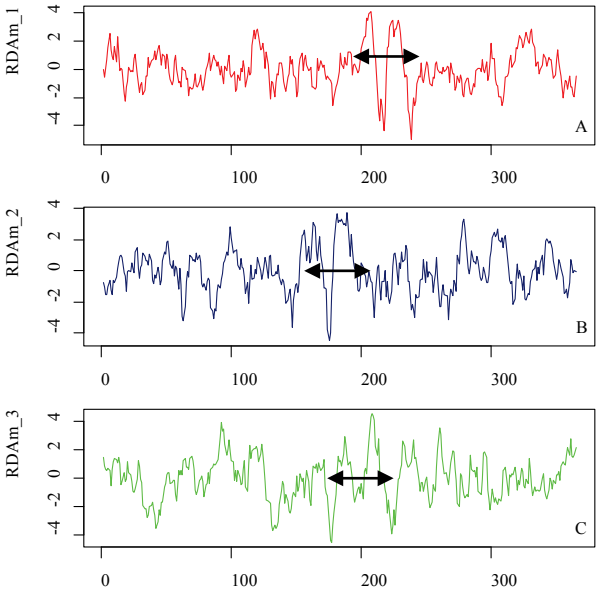


**Fig. 7.** The inter annual dynamic of the scores of the medium-scale components RDAm 1–3: *a* – the ordinate axis is the scores of the broad-scale components RDAm 1, *b* – RDAm 2, *c* – RDAm 3, the abscissa axis is the years within the period 1998–2018, the arrows show the time range with two consecutive drastic temperature changes

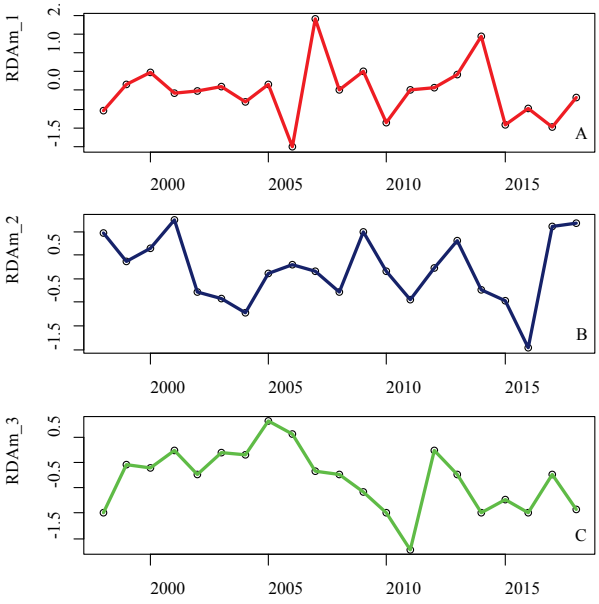


**Fig. 8.** The between annual dynamic of the scores of the medium-scale components RDAm 1–3: *a* – the ordinate axis is the scores of the broad-scale components RDAm 1, *b* – RDAm 2, *c* – RDAm 3, the abscissa axis is the years within the period 1998–2018, the arrows show the time range with two consecutive drastic temperature changes

The fine-scale axes characterize periods of the high-frequency temperature fluctuations that occur during a certain period of the season. Thus, RDAf 1 reflects the variability of the temperature regime in the period December-April (Fig. 9a), RDAf 2 – in November-May (Fig. 9b), RDAf 3 – in September-November and January/February (Fig. 9b). The degree of quantitative manifestation of the corresponding patterns by years is shown in Figure 10.

*Effect of temperature variation on the S. erythrophthalmus spawning.* Spawning of the *S. erythrophthalmus* began at 119–157 days of the year, ended at 139–157 days of the year (Table 1). The duration of spawning was 5–31 days. The temperature of water at the start of the spawning period was 14.0–18.4 °C. The distribution of spawning start time was symmetrical (Fig. 11). The distribution of spawning time was right-skewed asymmetrical (skewness was –0.49 ± 0.26). The distribution of spawning time and water temperature at the start of spawning were left-skewed asymmetrical (skewness was 0.60 ± 0.26 and 0.36 ± 0.26 respectively). The kurtosis for all, except the duration of spawning time, was negative, indicating that the distributions were bimodal. The kurtosis of spawning time duration was positive which reveals that corresponding distribution has heavier tails compared to the normal distribution.

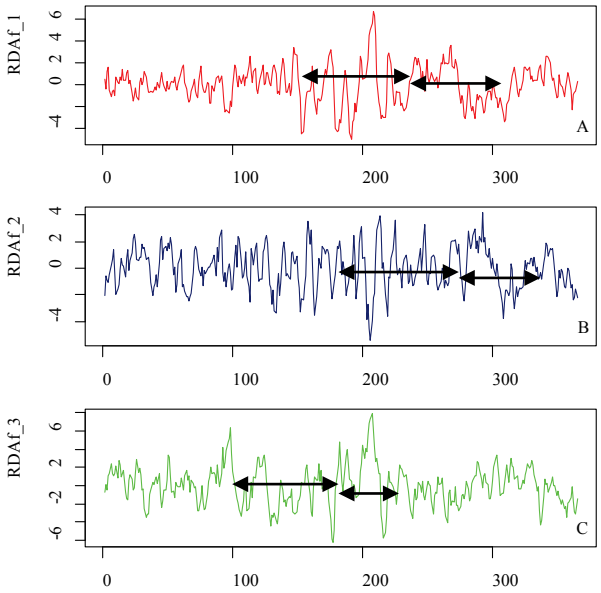


**Fig. 9.** The inter annual dynamic of the scores of the fine-scale components RDAf 1–3: *a* – the ordinate axis is the scores of the broad-scale components RDAf 1, *b* – RDAf 2, *c* – RDAf 3, the abscissa axis is the years within the period 1998–2018, the arrows show the time range with oscillating drastic temperature changes

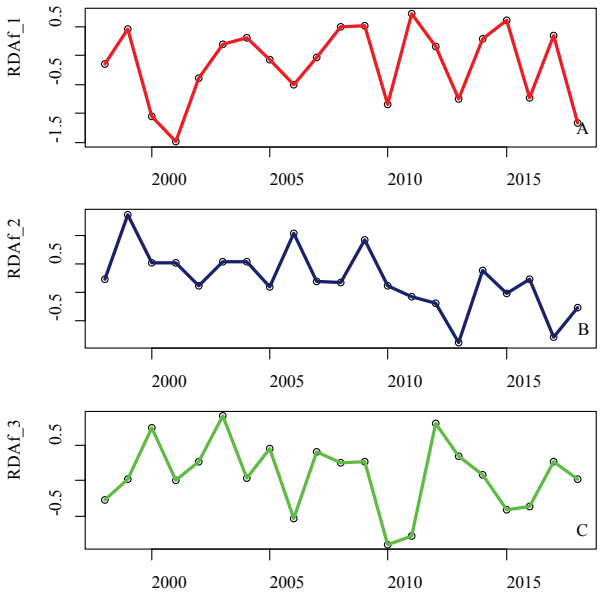


**Fig. 10.** The inter annual dynamic of the scores of the medium-scale components RDAm 1–3: *a* – the ordinate axis is the scores of the broad-scale components RDAf 1, *b* – RDAf 2, *c* – RDAf 3, the abscissa axis is the years within the period 1998–2018, the arrows show the time range with oscillating drastic temperature changes

The parameters of temperature dynamics and biotope type are able to explain 51–72% of variability of spawning event characteristics of *S. erythrophthalmus* (Table 2). The start of spawning is statistically significantly dependent on the broad-scale patterns (RDAb 2 and 3), medium-scale pattern RDAm 2 and fine-scale pattern RDAf 2 of temperature. The greater the amplitude of annual temperature fluctuations, the later spawning occurs. Of the biotopes, the earliest spawning occurs in the water bodies of the Protoch River system and Obukhov floodplain, and the latest in the water bodies of the River Dnipro (Fig. 12). The timing of ending of the spawning season depends on medium- and fine-scale patterns as well as phase shifts. The time of spawning in water bodies corresponds to the time of spawning start: the earlier spawning starts, the earlier it ends. The duration of the spawning season is influenced by the patterns of different scale levels, as well as the amplitude and shift of phases. In this case, the duration of spawning in all water bodies does not differ. Spawning temperature depends on medium- and fine-scale temperature patterns, but does not depend on the characteristics of the sinusoidal annual trend. Systematically lower water temperature at the beginning of the spawning season was observed in the Protoch River system and Obukhov floodplain, and systematically higher – in the Dnipro River.

**Table 1**
Descriptive statistics of the spawning characteristics of *Scardinius erythrophthalmus* for the period 1997–2018 (N = 84)

| Spawning characteristics | Mean ± SE | Median | Minimum | Maximum | Skewness ± SE | Kurtosis ± SE |
|---|---|---|---|---|---|---|
| Start of spawning, day | 132.8 ± 0.67 | 133 | 119 | 146 | 0.04 ± 0.26 | –0.72 ± 0.52 |
| End of spawning, day | 149.1 ± 0.51 | 150 | 139 | 157 | –0.49 ± 0.26 | –0.54 ± 0.52 |
| Duration of spawning, days | 16.3 ± 0.51 | 16 | 5 | 31 | 0.60 ± 0.26 | 0.89 ± 0.52 |
| Temperature of the water at the beginning of spawning | 15.9 ± 0.13 | 15.5 | 14.0 | 18.4 | 0.36 ± 0.26 | –0.74 ± 0.52 |

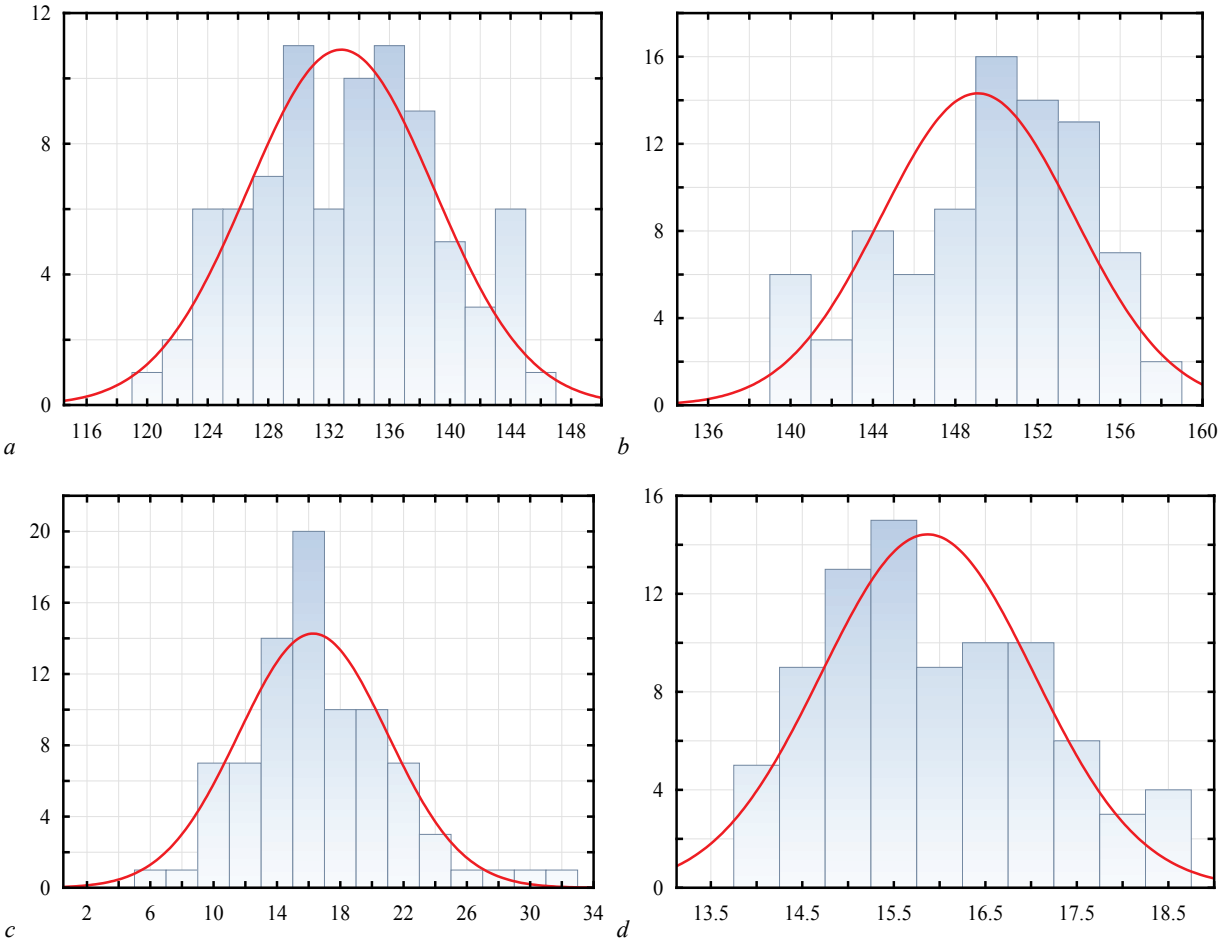


**Fig. 11.** Histogram of spawning characteristics: *a* – abscissa axis is the spawning start (number of days from the beginning of the year), *b* – abscissa axis is the spawning end (number of days from the beginning of the year), *c* – spawning duration (number of days), *d* – the water temperature at the time of start time spawning (°C), the ordinate is the density of distribution

## Discussion

The phenological rhythms of life dynamics of species is a form by which ecological systems reach stability of. Phenology affects nearly all aspects of ecology and evolution (Forrest & Miller-Rushing, 2010). To be successful, living organisms must coordinate their life cycles. Such coordination is the result of long evolutionary processes, and the the oscillatory processes in the environment are a regulatory factor (Bondarev et al., 2020; Fedushko et al., 2021). The ability to receive information from environmental factors to correct the rate of various stages of the life cycle is due to the regular repeatability of the rhythmic regimes of the environment. During the period of research we found that the average annual temperature does not affect the spawning time of *S. erythrophthalmus*. Therefore, the increasing temperature trend observed for the period 1998–2018 does not affect the spawning time. However, this is not a reason to argue that global climate change does not affect spawning dynamics. Understanding of the mechanisms of influence of climatic regimes on spawning phenology requires the identification of temperature fluctuation patterns during the year. We have established that such temperature patterns exist, but their characteristics do not fit into the traditional concepts of the hierarchy of oscillatory phenomena in living nature. The influence of oscillatory processes of different frequency is known: these are cycles of solar sunspot activity (Marques et al., 2015), annual cycles (circannual) (Gwinner, 1986), seasonal cycles, monthly cycles (circalunar) (Bondarev et al., 2018), half-monthly cycles (semi-lunar), tidal (circatidal) (Goto & Takekata, 2015; Raible et al., 2017), circadian cycles (Bulla et al., 2017).

To describe the spawning rhythm of *S. erythrophthalmus* we focused on the search for rhythmic processes in the range from a year to several days. We identified three groups of temperature oscillatory processes that take place during the year: broad-, medium- and detailed scale patterns. The temporal patterns within each group are qualitatively similar and the difference between them is mainly in phase shift. The most significant features of oscillatory dynamics cover the winter and spring periods of the year and such processes are reflected in fish spawning. The high frequency process, which covers autumn and winter events, had no significant impact on spawning events. Obviously, the rate of maturation of sexual products of *S. erythrophthalmus* depends largely on the rhythm of temperature during winter and spring, which affects the readiness of fish for spawning.

**Table 2**

The dependences of start, end, and duration of spawning of *Scardinius erythrophthalmus* and water temperature at the time of spawning on biotope type, temporal temperature patterns according to GLM-procedure (standardized regression coefficients ± SE)

| Predictors | Start of spawning, $R^2_a = 0.66$, $P < 0.001$ | End of spawning, $R^2_a = 0.72$, $P < 0.001$ | Duration of spawning, $R^2_a = 0.53$, $P < 0.001$ | Water temperature at the time of spawning, $R^2_a = 0.51$, $P < 0.001$ |
|---|---|---|---|---|
| Broad-scale temperature patterns | | | | |
| RDAb 1 | – | – | – | – |
| RDAb 2 | –0.22 ± 0.09 | – | 0.41 ± 0.11 | – |
| RDAb 3 | –0.41 ± 0.09 | – | 0.41 ± 0.11 | – |
| Medium-scale temperature patterns | | | | |
| RDAm 1 | – | – | – | – |
| RDAm 2 | –0.17 ± 0.07 | – | 0.18 ± 0.08 | –0.20 ± 0.08 |
| RDAm 3 | – | – | – | –0.33 ± 0.16 |
| Fine-scale temperature patterns | | | | |
| RDAf 1 | – | –0.22 ± 0.10 | –0.35 ± 0.13 | – |
| RDAf 2 | –0.32 ± 0.11 | – | 0.46 ± 0.13 | –0.33 ± 0.13 |
| RDAf 3 | – | – | – | – |
| Annual sinusoidal patterns | | | | |
| Temp* | – | – | – | – |
| A** | 0.39 ± 0.15 | – | –0.38 ± 0.15 | – |
| Phi*** | – | –0.26 ± 0.10 | –0.26 ± 0.11 | – |
| Biotope types (Biotope 4 as reference) | | | | |
| Biotope 1 | 0.36 ± 0.08 | 0.38 ± 0.07 | – | – |
| Biotope 2 | –0.66 ± 0.08 | –0.93 ± 0.07 | – | –0.36 ± 0.10 |
| Biotope 3 | 0.51 ± 0.08 | 0.52 ± 0.07 | – | 0.52 ± 0.10 |

*Note*: Temp* – average annual temperature; Biotope 1 – Nikolaev system of water bodies; Biotope 2 – Protoch River system and Obukhov floodplain; Biotope 3 – channel of the Dnipro River; Biotope 4 – water bodies of the Taromske ledge.

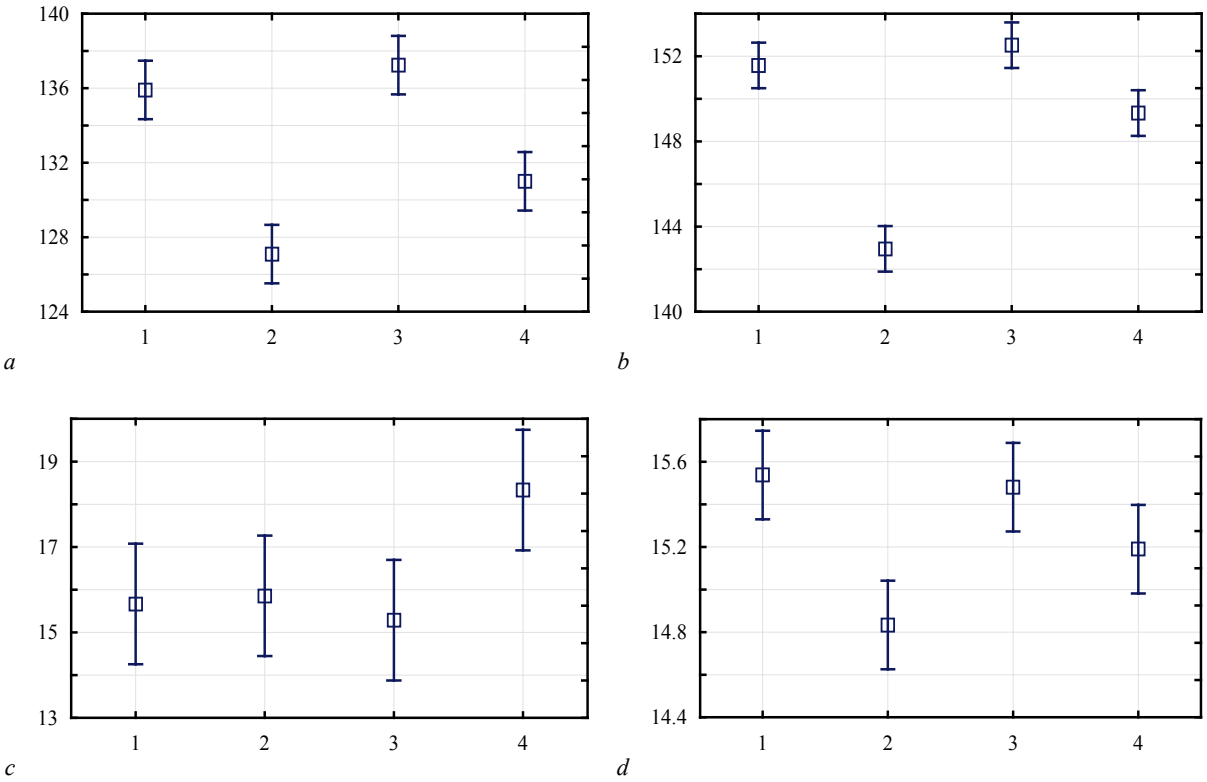


**Fig. 12.** Dependence of the onset time (*a*), the end (*b*) of spawning, spawning duration (*c*), water temperature at the time of spawning (*d*) on the type of biotope (mean and 95% confidence interval): *1* – Nikolaev ledge; *2* – Obuhovskiy floodplain, mouth of the Orel River; *3* – the Dnipro bed; *4* – Tarom ledge

The minimum water temperature of 14 ℃ determines the lower boundary at which spawning is possible in the studied water bodies. In the northern parts of the range, spawning is possible at lower temperatures (Boznak, 2008), while in the southern parts it is possible to spawn at higher temperatures (Tarkan, 2006). The onset of critical water temperature does not guarantee that spawning will start: spawning may occur at tem-

peratures as low as 18.4 ºC. In terms of time, this range, when spawning may occur, but does not, can cover 27 days. Critical water temperatures are different for different bodies of water, which also indicates the external regulation of spawning time.

The extracted patterns have a specific form, which fully manifests itself in the course of a year and can therefore be formally attributed to circannual cycles. However, the selected patterns are most sensitive to temperature changes over a period of time much shorter than the duration of the year. By their nature, these patterns have a complex hierarchical structure as a result of a combination of oscillatory processes of different frequency. In addition, the manifestation of these patterns is different from year to year. It is quite possible that long-term dynamics of degree of manifestation of temperature patterns of different scale has its own regularity of higher scale level.

The features of the pattern shape allow a meaningful interpretation of the nature of the influence of temperature regimes on spawning phenology. Thus, the time of occurrence of abrupt changes in temperature in February or December has a significant impact on the start date of spawning. Sharper relatively warmer weather and a sharp cooling in these months contribute to the earlier onset of spawning. Temperature fluctuations in the mean scale range during the period December to mid-January affect the start of spawning. The end time of spawning is characterized by a lower level of variation, so the variability in the duration of spawning depends more on the time of beginning, rather than end of spawning. Obviously, the values of regression coefficients for spawning time duration are opposite to the values of regression coefficients for spawning start time. Our results are in agreement with other studies. The spawning events of the white bream (*Blicca bjoerkna*) were explained by temperature variation of the current year up to the spawning event and by temperature variation in the preceding year. Climatic factors presented by the principal components were shown to have a significant explanatory power to describe the events of spawning of Prussian carp. Rapid warming in spring in combination with higher precipitation than normal can stimulate earlier spawning of this species (Zhukov et al., 2019).

The phenology of spawning events will take over from the rhythm of oscillatory processes of temperature change of different frequency throughout the year. The modeling of the phenological sequences is very important for enabling ecological forecasts in light of future climate change (Morisette et al., 2009). Global climate change is manifest not only in changes in mean annual temperature, but also in changes in the rhythm of natural processes during the year. Therefore, one of the mechanisms of influence on phenology of biological phenomena can be the variability of hierarchy of oscillatory processes of temperature regime.

The results obtained indicate the importance of conducting phenological studies in protected areas. Multi-year research provides information on the dynamics of environmental processes to clarify the role of global climate change with the possibility of creating long-term forecasts. Phenological research is conducted without removing animals from their habitats, which is especially important for research work within protected areas. The results lead to the question: are there regular patterns of variation in other climate indicators, such as precipitation? In the future, we plan to investigate the role of precipitation in fish spawning phenology.

## Conclusion

The annual course of temperatures can be decomposed into a sinusoidal trend, patterns of multiscale nature and a random fraction. The sinusoidal trend explained 78.3–87.6% of temperature variation. Sinusoidal trend depends on the average annual temperature, amplitude of temperature fluctuations during the year and earlier or later the seasons of the year (phase shift). Amplitude and phase shift play a role in describing spawning phenology. In the time range studied, the trend of average annual temperature increase was not statistically significant for spawning events. dbMEM variables were able to explain 72.7% variation of the sinusoidal trend residuals. This variation can be fractionated into broad-, medium and fine-scale components. Spawning start time was most sensitive to different scale temperature patterns. The greatest influence on spawning was made by oscillatory phenomena of the temperature regime in winter and spring before the start of spawning. Water temperature determines the lower possible limit of spawning start, but the real spawning start is determined by the preceding temperature dynamics.

## References


Alavi, S. M. H., & Cosson, J. (2005). Sperm motility in fishes. I. Effects of temperature and pH: A review. Cell Biology International, 29(2), 101–110.

Allen, C. R., Angeler, D. G., Garmestani, A. S., Gunderson, L. H., & Holling, C. S. (2014). Panarchy: Theory and application. Ecosystems, 17(4), 578–589.

Angeler, D. G., Viedma, O., & Moreno, J. M. (2009). Statistical performance and information content of time lag analysis and redundancy analysis in time series modeling. Ecology, 90(11), 3245–3257.

Avtaeva, T., Petrovičová, K., Langraf, V., & Brygadyrenko, V. (2021). Potential bioclimatic ranges of crop pests *Zabrus tenebrioides* and *Harpalus rufipes* during climate change conditions. Diversity, 13(11), 559.

Baho, D. L., Futter, M. N., Johnson, R. K., & Angeler, D. G. (2015). Assessing temporal scales and patterns in time series: Comparing methods based on redundancy analysis. Ecological Complexity, 22, 162–168.

Berg, L. S. (1949). Fishes of fresh waters of the USSR and adjacent countries. Vol. 2. AN SSSR, Moscow, Leningrad.

Billard, R. (1986). Spermatogenesis and spermatology of some teleost fish species. Reproduction Nutrition Développement, 26(4), 877–920.

Billard, R., Breton, B., Fostier, A., Jalabert, B., & Weil, C. (1978). Endocrine control of the teleos reproductive cycle and its relation to external factors: Salmonid and cyprinid models. In: Gaillard, H. H. B. P. J. (Ed.). Comparative endocrinology. North Holland Biomedical Press, Amsterdam. Pp. 37–47.

Black, B. A., Schroeder, I. D., Sydeman, W. J., Bograd, S. J., & Lawson, P. W. (2010). Wintertime ocean conditions synchronize rockfish growth and seabird reproduction in the Central California current ecosystem. Canadian Journal of Fisheries and Aquatic Sciences, 67(7), 1149–1158.

Blanchet, F. G., Bergeron, J. A. C., Spence, J. R., & He, F. (2013). Landscape effects of disturbance, habitat heterogeneity and spatial autocorrelation for a ground beetle (Carabidae) assemblage in mature boreal forest. Ecography, 36(5), 636–647.

Bondarev, D. L., Fedyushko, M. P., Gubanova, N. L., & Zhukov, O. V. (2020). The temporal dynamic of young fish communities in the water bodies of the "Dnipro-Orylskiy" Nature Reserve. Agrology, 3(3), 145–159.

Bondarev, D., Fedushko, M., Hubanova, N., Novitskiy, R., Kunakh, O., & Zhukov, O. (2022). Temporal dynamics of the fish communities in the reservoir: The influence of eutrophication on ecological guilds structure. Ichthyological Research, in press.

Bondarev, D., Kunakh, O., & Zhukov, O. (2018). Assessment of the impact of seasonal patterns climatic conditions on spawning events of the white bream *Blicca bjoerkna* (Linnaeus, 1758) in astronomical and biological time. Acta Biologica Sibirica, 4(2), 61.

Borcard, D., & Legendre, P. (2002). All-scale spatial analysis of ecological data by means of principal coordinates of neighbour matrices. Ecological Modelling, 153, 51–68.

Boznak, E. I. (2008). The rudd *Scardinius erythrophthalmus* from tributaries of the Northern Dvina. Journal of Ichthyology, 48(5), 408–410.

Breton, B., Horoszewicz, L., Billard, R., & Bieniarz, K. (1980). Temperature and reproduction in tench: Effect of a rise in the annual temperature regime on gonadotropin level, gametogenesis and spawning. I. The male. Reproduction Nutrition Développement, 20(1A), 105–118.

Brett, J. R. (1979). Environmental factors and growth. In: Hoar, W. S., Randall, D. J., & Brett, J. R. (Eds.). Fish physiology. Vol. 8: Bioenergetics and growth. Academic Press, New York, London. Pp. 599–675.

Bulakhov, V. L., Novitsky, R. O., Pakhomov, O. E., & Khristov, O. O. (2008). Biological diversity of Ukraine. Dnipropetrovsk region. Cyclostomes (Cyclostomata). Fishes (Pisces). Dnipropetrovsk University Press, Dnipropetrovsk.

Bulla, M., Oudman, T., Bijleveld, A. I., Piersma, T., & Kyriacou, C. P. (2017). Marine biorhythms: Bridging chronobiology and ecology. Philosophical Transactions of the Royal Society B: Biological Sciences, 372(1734), 20160253.

Chavez, F. P., Ryan, J., Lluch-Cota, S. E., & Ñiquen, C. M. (2003). From anchovies to sardines and back: Multidecadal change in the Pacific Ocean. Science, 299(5604), 217–221.

Cooper, S. D., Diehl, S., Kratz, K., & Sarnelle, O. (1998). Implications of scale for patterns and processes in stream ecology. Austral Ecology, 23(1), 27–40.

Domagała, J., Kirczuk, L., & Pilecka-Rapacz, M. (2013). Annual development cycle of gonads of Eurasian ruffe (*Gymnocephalus cernuus* L.) females from lower Odra River sections differing in the influence of cooling water. Journal of Freshwater Ecology, 28(3), 423–437.

Dray, S., Legendre, P., & Peres-Neto, P. R. (2006a). Spatial modelling: A comprehensive framework for principal coordinate analysis of neighbour matrices (PCNM). Ecological Modelling, 196, 483–493.

Fedushko, M. P., Bondarev, D. L., Gubanova, N. L., & Zhukov, O. V. (2021). Effects of eutrophication on the long-term dynamics of juvenile fish communities. Agrology, 4(4), 149–164.

Forrest, J., & Miller-Rushing, A. J. (2010). Toward a synthetic understanding of the role of phenology in ecology and evolution. Philosophical Transactions of the Royal Society B: Biological Sciences, 365(1555), 3101–3112.
Gao, J., Hu, J., & Wen Tung, W. (2011). Facilitating joint chaos and fractal analysis of biosignals through nonlinear adaptive filtering. PLoS One, 6(9), e24331.
Gao, J., Hu, J., Mao, X., & Perc, M. (2012). Culturomics meets random fractal theory: Insights into long-range correlations of social and natural phenomena over the past two centuries. Journal of The Royal Society Interface, 9(73), 1956–1964.
Garcia, A. M., Vieira, J. P., Winemiller, K. O., Moraes, L. E., & Paes, E. T. (2012). Factoring scales of spatial and temporal variation in fish abundance in a subtropical estuary. Marine Ecology Progress Series, 461, 121–135.
Goto, S. G., & Takekata, H. (2015). Circatidal rhythm and the veiled clockwork. Current Opinion in Insect Science, 7, 92–97.
Gwinner, E. (1986). Evidence for circannual rhythms. In: Bradshaw, S. D., Burggren, W., Heller, H. C., Ishii, S., Langer, H., Randall, D. J., & Neuweiler, G. (Eds.). Zoophysiology. Springer. Pp. 11–38.
Herzig, A., & Winkler, H. (1986). The influence of temperature on the embryonic development of three cyprinid fishes, *Abramis brama*, *Chalcalburnus chalcoides mento* and *Vimba vimba*. Journal of Fish Biology, 28(2), 171–181.
Jafri, S. (1989). The effects of photoperiod and temperature manipulation on reproduction in the roach, *Rutilus rutilus* (L.) (Teleostei). Pakistan Journal of Zoology, 213, 289–299.
Jobling, M. (2003). The thermal growth coefficient (TGC) model of fish growth: A cautionary note. Aquaculture Research, 34(7), 581–584.
Kennedy, M., & Fitzmaurice, P. (1974). Biology of the rudd *Scardinius erythrophthalmus* (L.) in Irish Waters. Proceedings of the Royal Irish Academy. Section B: Biological, Geological, and Chemical Science, 74(18), 245–303.
Kodba, S., Perc, M., & Marhl, M. (2005). Detecting chaos from a time series. European Journal of Physics, 26(1), 205.
Korzelecka, A., & Winnicki, A. (1998). Peculiarities of embryogenesis in *Scardinius erythrophthalmus* L. Electronic Journal of Polish Agricultural Universities. Series Fisheries, 1, 1.
Koshelev, O., Koshelev, V., Fedushko, M., & Zhukov, O. (2021). Annual course of temperature and precipitation as proximal predictors of birds' responses to climatic changes on the species and community level. Folia Oecologica, 48(2), 118–135.
Kottelat, M., & Freyhof, J. (2007). Handbook of European freshwater fishes. Maurice Kottelat, Cornol, Switzerland.
Lahnsteiner, F., & Mansour, N. (2012). The effect of temperature on sperm motility and enzymatic activity in brown trout *Salmo trutta*, burbot *Lota lota* and grayling *Thymallus thymallus*. Journal of Fish Biology, 81(1), 197–209.
Legendre, P., & Legendre, L. (2012). Canonical analysis. Developments in Environmental Modelling, 24(C), 625–710.
Levin, S. A. (1992). The problem of pattern and scale in ecology: The Robert H. Mac Arthur award lecture. Ecology, 73(6), 1943–1967.
Marques, L. V., Short, F. T., & Creed, J. C. (2015). Sunspots drive seagrasses. Biological Rhythm Research, 46(1), 63–68.
McGowan, J. A., Cayan, D. R., & Dorman, L. M. (1998). Climate-ocean variability and ecosystem response in the Northeast Pacific. Science, 281(5374), 210–217.
Morisette, J. T., Richardson, A. D., Knapp, A. K., Fisher, J. I., Graham, E. A., Abatzoglou, J., Wilson, B. E., Breshears, D. D., Henebry, G. M., Hanes, J. M., & Liang, L. (2009). Tracking the rhythm of the seasons in the face of global change: Phenological research in the 21st century. Frontiers in Ecology and the Environment, 7(5), 253–260.
Nash, K. L., Allen, C. R., Angeler, D. G., Barichievy, C., Eason, T., Garmestani, A. S., Graham, N. A. J., Granholm, D., Knutson, M., Nelson, R. J., Nyström, M., Stow, C. A., & Sundstrom, S. M. (2014). Discontinuities, cross-scale patterns, and the organization of ecosystems. Ecology, 95(3), 654–667.
Nõges, P., & Järvet, A. (2005). Climate driven changes in the spawning of roach (*Rutilus rutilus* (L.)) and bream (*Abramis brama* (L.)) in the Estonian part of the Narva River basin. Boreal Environment Research, 10(1), 45–55.
Papageorgiou, N., & Neophytou, C. (1982). Age, growth and fecundity of the rudd (*Scardinius erythrophthalmus* L.) in Lake Kastoria. Thalassographica, 2, 5–15.
Patimar, R., Nadjafypour, E., Yaghouby, M., & Nadjafy, M. (2010). Reproduction characteristics of a stunted population of rudd, *Scardinius erythrophthalmus* (Linnaeus, 1758) living in the Anzali Lagoon (the Southwest Caspian Sea, Iran). Journal of Ichthyology, 50(11), 1060–1065.
Perry, A. L., Low, P. J., Ellis, J. R., & Reynolds, J. D. (2005). Climate change and distribution shifts in marine fishes. Science, 308(5730), 1912–1915.
Raible, F., Takekata, H., & Tessmar-Raible, K. (2017). An overview of monthly rhythms and clocks. Frontiers in Neurology, 8(5), 1–14.
Rheinberger, V., Hofer, R., & Wieser, W. (1987). Growth and habitat separation in eight cohorts of three species of cyprinids in a subalpine lake. Environmental Biology of Fishes, 18(3), 209–217.
Sandstrom, O., Neuman, E., & Thoresson, G. (1995). Effects of temperature on life history variables in perch. Journal of Fish Biology, 47(4), 652–670.
Scheffer, M., & Van Nes, E. H. (2007). Shallow lakes theory revisited: Various alternative regimes driven by climate, nutrients, depth and lake size. Hydrobiologia, 584(1), 455–466.
Schneider, K. N., Newman, R. M., Card, V., Weisberg, S., & Pereira, D. L. (2010). Timing of walleye spawning as an indicator of climate change. Transactions of the American Fisheries Society, 139(4), 1198–1210.
Shikhshabekov, M. M. (1979). The reproductive biology of the "kutum", *Rutilus frisii kutum*, the asp, *Aspius aspius*, the vimba, *Vimba vimba persa*, and the rudd, *Scardinius erythrophthalmus*, in the waters of Dagestan. Journal of Ichthyology, 19, 98–105.
Stehlik, J. (1968). Fecundity of *Scardinius erythrophthalmus* L. Acta Musei Silesiae, 17, 81–88.
Tarkan, A. S. (2006). Reproductive ecology of two cyprinid fishes in an oligotrophic lake near the southern limits of their distribution range. Ecology of Freshwater Fish, 15(2), 131–138.
Vejříková, I., Vejřík, L., Syväranta, J., Kiljunen, M., Čech, M., Blabolil, P., Vašek, M., Sajdlová, Z., Chung, S. H. T., Šmejkal, M., Frouzová, J., & Peterka, J. (2016). Distribution of herbivorous fish is frozen by low temperature. Scientific Reports, 6(1), 1–11.
Vila-Gispert, A., & Moreno-Amich, R. (2000). Fecundity and spawning mode of three introduced fish species in Lake Banyoles (Catalunya, Spain) in comparison with other localities. Aquatic Sciences, 62(2), 154–166.
Vislocky, R. L., & Fritsch, J. M. (1995). Generalized additive models versus linear regression in generating probabilistic MOS forecasts of aviation weather parameters. Weather and Forecasting, 10(4), 669–680.
Weijerman, M., Lindeboom, H., & Zuur, A. (2005). Regime shifts in marine ecosystems of the North Sea and Wadden Sea. Marine Ecology Progress Series, 298, 21–39.
Zerunian, S., Valentini, L., & Gibertini, G. (1986). Growth and reproduction of rudd and red-eye roach (Pisces, Cyprinidae) in Lake Bracciano. Bolletino Di Zoologia, 53(1), 91–95.
Zhukov, O. V., Bondarev, D. L., Yermak, Y. I., & Fedushko, M. P. (2019). Effects of temperature patterns on the spawining phenology and niche overlap of fish assemblages in the water bodies of the Dnipro River basin. Ecologica Montenegrina, 22, 177–203.